REGULATION OF THE INNATE IMMUNE RESPONSES AUTOPHAGY AND INFLAMMASOME ACTIVATION DURING BACTERIAL INFECTION

by

Jennie Vorhauer

BS, Allegheny College, 2014

Submitted to the Graduate Faculty of

School of medicine in partial fulfillment

of the requirements for the degree of

Master of Science

University of Pittsburgh

2017

UNIVERSITY OF PITTSBURGH

School of Medicine

This thesis was presented

by

Jennie Vorhauer

It was defended on

June 24, 2017

and approved by

Wendy Mars, Associate Professor, Department of Pathology

Melanie Scott, Assistant Professor, Department of Pathology, Department of Surgery

Nahed Ismail, Professor, Department of Pathology

REGULATION OF THE INNATE IMMUNE RESPONSES AUTOPHAGY AND INFLAMMASOME ACTIVATION DURING BACTERIAL INFECTION

Jennie Vorhauer, M.S.

University of Pittsburgh, 2017

Autophagy is an innate anti-microbial host defense that maintains tissue homeostasis. Autophagy is negatively regulated by the nutrient-sensing mTORC1 complex. In this study, we examined the regulatory mechanisms of autophagy and inflammasome activation during *Ehrlichia* infection. Monocytic *Ehrlichia* is a Gram negative intracellular bacterial pathogen that causes fatal human monocytic ehrlichiosis. *Ehrlichia* lacks LPS, but induces inflammasome activation leading to acute liver damage. In humans, the potentially fatal human monocytic ehrlichiosis (HME) mimics sepsis and toxic shock-like syndrome [1, 2], making *Ehrlichia* a viable model system for these conditions in the absence of LPS. During virulent *Ehrlichia* infection confocal data shows that autophagy increased with infection, despite clear activation of the autophagy inhibitor mTORC1. This is likely due to a balance of mTORC1 dependent and independent autophagy. Employing bone marrow derived macrophages (BMM) from mice deficient in MyD88 and TLR9 we reveal a novel signaling pathway for IOE mediated autophagy regulation and inflammasome activation centered around IFNβ production. We have previously shown that the virulent *Ehrlichia* strain *Ixodes ovatus Ehrlichia* (IOE) expresses higher levels of IFNβ than the avirulent strain *Ehrlichia muris* (EM) [3]. When IFNβ is added to BMM mTORC1 activation increases, a phenomenon further increased when IFNβ is added to IOE infected BMM. Both IOE and IFNβ mediated mTORC1 activation are abrogated by knockout of the TLR9 receptor. This placed IFNβ upstream of TLR9 in the IOE mediated mTORC1 signaling pathway. As both TLR9 is activated by dsDNA, we have hypothesized that these receptors are activated

are activated by mitochondrial DNA released in response to IFNβ mediated DAMP production. These data suggest that LPS-negative *Ehrlichia* regulates autophagy with mTORC1, and that this mTORC1 activation is achieved via IFNβ mediated TLR9. Our findings reveal a novel regulation of autophagy and the inflammasome in macrophages via MyD88 and mTORC1 during infection with intracellular pathogens.

TABLE OF CONTENTS

LIST OF FIGURES

1.0 INTRODUCTION

We examined the effect of bacterial infection on inflammasome activation and autophagy in *murine* primary macrophages using *Ixodes ovatus Ehrlichia* (IOE); a Gram negative obligate intracellular bacterium lacking lipopolysaccharide (LPS). We show that IOE infection in macrophages results in MYD88-dependent mTOR activation and inhibition of autophagy flux, a response enhanced by IFNb stimulation. Additionally, MYD88 is critical for IOE induced inflammasome activation, including increases in TNF-α and IL-1β production.

1.1 EHRILICHIA AND THE INNATE IMMUNE RESPONSE

Ehrlichia is an obligate intracellular gram-negative bacteria which primarily proliferates in monocytes and macrophages, resides in endosomal compartments, and also infects hepatic and splenic tissue [4]. The emerging infectious disease Human Monocytotropic Ehrlichiosis (HME) results from infection with the human specific *Ehrlichia* strain *Ehrlichia chaffeensis* [5]. HME severity varies dramatically, from asymptomatic to fatal toxic-shock-like syndrome with multi-organ failure [6]. The clinical and pathological manifestations of HME closely resemble those observed in the *murine* model of fatal Ehrlichiosis infection with the highly virulent strain (IOE), making *murine* IOE infection an excellent model for studies of HME. Additionally, *Ehrlichia*

lacks the lipopolysaccharide (LPS) and peptidoglycan classically produced by gram negative bacteria. To maintain outer membrane integrity *Ehrlichia* instead acquires cholesterol from the host cell membrane [7]. This makes *Ehrlichia* more applicable as a broader model system compared to any LPS producing bacteria, which will produce an immune response largely dependent on the toxicity of LPS. *Ehrlichia* species employ various mechanisms to evade host immune responses and proliferate within the cell, thus facilitating bacterial dissemination. For example, *Ehrlichia chaffeensis* directly inhibits production of cytokines such as IL-12 and IFNγ, which are involved in cell-mediated defense against intracellular bacteria [8].

Innate immune cells respond to pathogen-associated factors via expression of toll-like receptors (TLRs) and cytosolic nucleotide-binding oligomerization domain-like receptors (NLRs). TLRs and NLRs represent a group of pattern recognition receptors (PRRs) which are critical to both host innate immune response, and adaptive immune response [9]. TLRs and NLRs recognize and respond to a variety of pathogen associated molecular patterns (PAMPs) [10]such as LPS, lipoproteins, nucleic acids, and danger associated molecular patterns (DAMPs) [11] such as ROS. Recognition of PAMPS or DAMPS by NLRs triggers the assembly of inflammasomes. Inflammasomes are multiprotein complexes necessary for the maturation of inflammatory cytokines such as IL-1β or IL-18 [9].

Inflammatory responses can be broken down into two broad categories, canonical and non-canonical. These categories are distinguished primarily by the active caspase, component which is cleaved and integrated into the resulting inflammasome complex. Canonical inflammatory response leads to direct caspase 1 activation, where as non-canonical inflammatory response results in activation of caspase 11 [12] in mice or its human analog caspase 4 [13].

These TLRs then activate the downstream molecules MyD88 or TRIF [14], which elicit a signaling cascade that induces inflammasome activation, and inhibits autophagy. We have chosen to focus on TLR9 and MyD88 as both display increased mRNA levels in IOE infected macrophages. This induction is likely tied to IOE's high virulence, as IOE mediated MyD88 and TLR9 expression is significantly higher than that induced by the less virulent *Ehrlichia* strain *Ehrlichia muris* (EM). TLR9 senses bacterial DNA in the endosome, as well as fragmented mitochondrial DNA released as a byproduct of cell damage [15]. It is possible that other TLRs also play a lesser role in IOE dependent TLR signaling, except for the LPS-sensing TLR4 [16], but TLR9 appears to play a primary role in IOE mediated cell signaling.

1.2 AUTOPHAGY

Innate host response utilizes autophagy to eliminate intracellular pathogens, thus autophagy may mediate IOE clearance. Autophagy is a metabolic function which can also act as an immune effector to mediate pathogen clearance [17]. During autophagy, damaged cell components are encased in membranous autophagosomes. These autophagosomes then fuse with lysosomes, and the cargo is degraded by the contents of the highly acidic lysosome. The regulatory mechanisms for autophagy are very complex, but in general terms autophagy can be broken down in to three basic steps: induction, elongation, and fusion/degradation [17]. When studying autophagy, the progression through these steps is often characterized by the lipidation state of the protein LC3, otherwise known as the conversion of LC3I to LC3II. During elongation, when the potential autophagosomes membrane expands and closes, LC3I is brought to the autophagosome membrane by the autophagy facilitator protein ATG3. Once LC3I binds to the autophagosomal

membrane it becomes lipidated, the molecular weight of the protein changes, and this new compound can be used to track the autophagosome through the processes of autophagosome formation, fusion with the lysosome, and degradation [18-20]. For this study, we have focused on mTORC1 activation as determined by phosphorylation of the ribosomal protein S6, which inhibits autophagosome membrane formation, as well as lipidation, localization, and degradation of the autophagy proteins p62 and LC3.

1.2.1 mTORC dependent autophagy

Mammalian target of rapamycin complex 1 (mTORC1), a member of the phosphoinositide 3-kinase PI3K family, is a negative regulator of autophagy. mTOR kinase signaling acts as an integration point for various TLR and cytokine receptor signals in the immune microenvironment. Many cellular signals converge on mTOR complex 1 (mTORC1) to regulate autophagy induction, or the formation of the initial autophagosomal membrane[18]. This includes signaling through the mTORC2 dependent serine/threonine kinase Akt. Phosphorylation of Akt modulates autophagic activity regulated through the PI3K pathway. Activation of the metabolic sensor mTOR, specifically the complex mTORC1, blocks autophagy flux by inhibiting the complexing of beclin-1 and ULK which are essential proteins for autophagosome formation [21]. mTORC1 is inhibited by amino acid starvation and cell stress as mechanisms for increasing autophagy during times of metabolic need. This mechanism may also be employed to contain and destroy bacteria in infected cells. We employ IOE as a broad model for innate immune response.

1.2.2 mTORC independent autophagy

mTORC independent autophagy occurs through one of three known pathways: Ca^{2+}/calpan, cAMP/Epac/Inositol, and JNK1/Beclin-1/PI_3KC_3 [22]. Similar to mTORC dependent autophagy, mTORC independent autophagy has been shown in both infected and naïve cells, with both naive *Atp6ap2* knockout hepatocytes and bluetounge virus (BVT) infected cells displaying simultaneous mTORC1 activation and high autophagy rates [23]·[24] as shown by confocal microscopy and LC3 accumulation respectively. In our system mTOR independent autophagy through the calpan pathway seems most probably, as the Ca^{2+} sensing inherent in this pathway provides a clear connection to *Ehrlichia* pathology [25], as well as a potential avenue for intervention through mitochondrial damage [26]. This study provides novel distinct regulation of autophagy and inflammasome by MyD88 in different target cells employing a non LPS-bacterial infection model.

2.0 MATERIALS AND METHODS

2.1 ETHICS STATEMENT

This study was carried out in strict accordance with the recommendations in the Guide for the Care and Use of Laboratory Animals of the National Institutes of Health. The protocol was approved by the Committee on the Ethics of Animal Experiments of the University of Pittsburgh in accordance with the institutional guidelines for animal welfare.

2.2 MICE AND *EHRLICHIA* INFECTION

Female 8 to 12 weeks old mice of the C57Bl/6 background deficient in TLR 9 (TLR 9-/-) as well as wild type (WT) mice were obtained from Jackson Laboratories (Bar Harbor, ME). All animals were housed under specific pathogen-free conditions at the Animal Research Facility in the University of Pittsburgh.

The highly virulent monocytic strain of *Ehrlichia, Ixodes ovatus Ehrlichia* (IOE) was provided by Dr. Yasuko Rikihisa (Ohio State University, Columbus, OH). IOE stock was propagated by passage through wild type C57BL/6 mice. Single-cell suspensions from spleens harvested from mice 7 days post-infection (p.i.) were stored in sucrose and potassium phosphate (SPK) buffer (0.5 M K_2HPO_4, 0.5 M KH_2PO_4, and 0.38 M sucrose) in liquid nitrogen and used as stocks. Mice were infected by intraperitoneal (i.p.) injection with a high dose of IOE (10^3-10^4 organisms/mouse). At 7 days p.i., mice per group were sacrificed, and spleens and livers

were harvested for further analysis. For survival experiments, mice were monitored daily for signs of illness and survival.

2.3 ISOLATION AND INFECTION OF BONE MARROW DERIVED MACROPHAGES

Bone marrow was isolated as previously described [27] from naive WT, TLR2-/-, TLR9-/-, and STING-/- mice. Briefly, femurs were excised and flushed under aseptic conditions. Bone marrow cells were seeded in 100 mm petri dishes at $1x10^5$ cells/10 ml/dish in DMEM/F12-GlutaMAX (Invitrogen) supplemented with 10% FBS (Invitrogen), 20 ng/ml MCSF (PeproTech), 10 mM Hepes (Invitrogen), and 10 mM glutamine (Invitrogen). Approximately 4 ml of fresh media was added after 3 days of culture. On day 6, cells were collected and the number of BMM was determined by flow cytometry and staining with fluorophore conjugated antibodies specific to CD11b and CD11c. The number of CD11c-CD11b+ BMM isolated by this method was ~ 95%. BMM collected on day 6 were seeded into 12 well plates for 20 h prior to infection at a density of 10^6 cells/well in DMEM/F12 (Invitrogen) supplemented with 5% FBS, 20 ng/ml MCSF, 10 mM Hepes.

Cell-free IOE organisms were prepared from IOE-infected splenocytes as previously described (Ismail, et al, 2004JI). IOE organisms were added to the BMM cultures at multiplicity of infection (MOI) of 0.5. When indicated, cells were pretreated for 1 h with recombinant IFNβ (400 units/ml), in the presence or absence of IOE. Cells were collected 24 h post-infection, and protein extracted for further analysis by western blot. Supernatants were collected and stored at −80°C for cytokine analysis.

2.4 BACTERIAL BURDEN MEASUREMENT USING QUANTITATIVE REAL-TIME PCR

Total DNA was isolated from liver and spleen tissues using the DNeasy Blood and Tissue kit (QIAGEN). Bacterial burden was determined using an iCycler IQ multicolor real-time detection system (Bio-Rad Laboratories, Hercules, CA) and primers and probes for the IOE *dsb* gene as previously described (Stevenson et al). The primers and probes used are as follows: IOE *dsb* forward: 5′-CAG GAT GGT AAA GTA CGT GTG A-3′; IOE *dsb* reverse: 5′- TAG CTA AYG CTG CCT GGA CA-3′; IOE probe: (6FAM)-AGG GAT TTC CCT ATA CTC GGT GAG GC-(MGB-BHQ). The eukaryotic housekeeping gene *gapdh* was amplified using the following primers/probes: GAPDH forward: 5′-CAA CTA CAT GGT CTA CAT GTT C-3′; GAPDH reverse: 5′-TCG CTC CTG GAA GAT G-3'; GAPDH probe: (6FAM)-CGG CAC AGT CAA GGC CGA GAA TGG GAA GC-(MGB-BHQ). The comparative cycle threshold (C_T) method was used to determine the bacterial burden. The results were normalized to the levels of expression of the *gapdh* in the same sample and expressed as copy number per 10^4 copies of *gapdh*. The results were considered negative for *Ehrlichia* DNA if $C_T \geq 38$ in the PCR reaction.

2.5 MEASUREMENT OF CYTOKINE LEVELS BY ENZYME-LINKED IMMUNOSORBENT ASSAY

The levels of IL-1β, and TNF-α in serum of infected mice or produced by the knockout and WT control BMM in culture supernatants were determined by commercially available enzyme-linked

immunosorbent assay (ELISA (eBioscience, San Diego, CA; Vienna, Austria)) kits according to the manufacturer's instructions.

2.6 PROTEIN EXTRACTION AND WESTERN BLOT ANALYSIS

Liver tissues and BMMs were lysed in T-PER lysis buffer or RIPA buffer (Thermo Fisher Scientific, Waltham, MA), respectively, supplemented with protease inhibitors and 1 mM phenylmethylsulphonyl fluoride (PMSF). Cell debris was removed by centrifugation. Protein extraction was performed at 4°C for 30 min. The protein content of the lysates was measured using a Bicinchoninic Acid Assay Kit (Pierce). Lysates (15-30 ug) were resolved in 4% to 20% gradient SDS–PAGE under reducing conditions. After electrophoresis, proteins were transferred onto PVDF membranes (BioRad) and blocked for 1 h in Tris-buffered saline (TBS) containing 5% non-fat milk and 0.1% Tween 20. Blots were probed with the appropriate primary antibodies and peroxidase-conjugated bovine anti-rabbit secondary antibodies (1:10000) (Santa Cruz Biotechnology). The membranes were processed and probed with the following antibodies, according to standard protocols: anti–caspase-1 (2 μg/mL) (EMD Millipore, Billerica, MA); anti-LC3B (dilution 1:1000) (Sigma-Aldrich, St. Louis, MO). Specific signals were developed using the ECL-Plus system (GE). Blots were stripped with Restore Western Blot Stripping Buffer (Pierce) and re-probed with GAPDH (dilution 1:5000). Mean pixel density of bands in Western blots was determined using ImageJ software version 1.48 (NIH, Bethesda, MD).

2.7 HISTOPATHOLOGY AND TERMINAL DEOXYNUCLEOTIDYL TRANSFERASE D-UTP NICK END LABELING (TUNEL) ASSAY

Tissue sections were fixed in a 10% solution of neutral buffered formalin, dehydrated in graded alcohols, embedded in paraffin wax, and stained with hematoxylin and eosin (H&E). Semi-quantitative analysis of the liver lesions was carried out using three parameters: the number of necrotic cells, the number of apoptotic cells, and the number of inflammatory foci in each high-power field (HPF). TUNEL staining was performed on unstained tissue sections, showing apoptotic cell death without focal necrosis, as described previously.

2.8 STATISTICAL ANALYSIS

All the data presented are representative of two or three independent experiments that yielded similar results. Two groups analysis was performed using an unpaired two-tailed *t* test. For comparison of multiple experimental groups, we used one –way analysis of variance (ANOVA) with Bonferroni's procedure. To determine whether the difference in survival between different mice groups was significant, data were analyzed by the Breslow-Wilcoxon Test. All statistical analyses were performed using GraphPad Prism (GraphPad Software Inc., La Jolla, CA, USA). Data are represented by means and standard deviations (SD). Differences with *P* values of 0.05, 0.01, and 0.001 were considered slightly (*), moderately (**), and highly (***) significant, respectively.

3.0 RESULTS

3.1 MYD88 SIGNALING PROMOTES *EHRLICHIA*-INDUCED IMMUNOPATHOLOGY AND SUSCEPTIBILITY TO FATAL *EHRLICHIOSIS*

Ehrlichia-induced toxic shock is caused by immunopathology and excessive inflammation [8, 28, 29]. To investigate the role of MyD88 in the pathogenesis of ehrlichiosis, we analyzed host response to *Ehrlichia* in WT and MyD88$^{-/-}$ mice infected with a high dose of IOE. 100% of IOE-infected WT mice succumbed to lethal infection on days 7-9 post-infection (p.i.) In contrast, ~70% of MyD88$^{-/-}$ mice succumbed to infection at that time point (P=0.0084) (Fig. 1A), and these mice have a significantly higher bacterial burden in the liver on day 7 p.i. when compared to WT mice (Fig. 1B). Interestingly, the lack of MyD88 signaling attenuated liver injury as evidenced by significantly decreased apoptotic (TUNEL positive) hepatocytes and Kupffer cells. Further, H&E staining demonstrated reduced magnitude of fatty changes/steatosis and necrosis in the liver of infected MyD88$^{-/-}$ mice (as shown by H&E staining) when compared to WT mice (Fig. 1C).

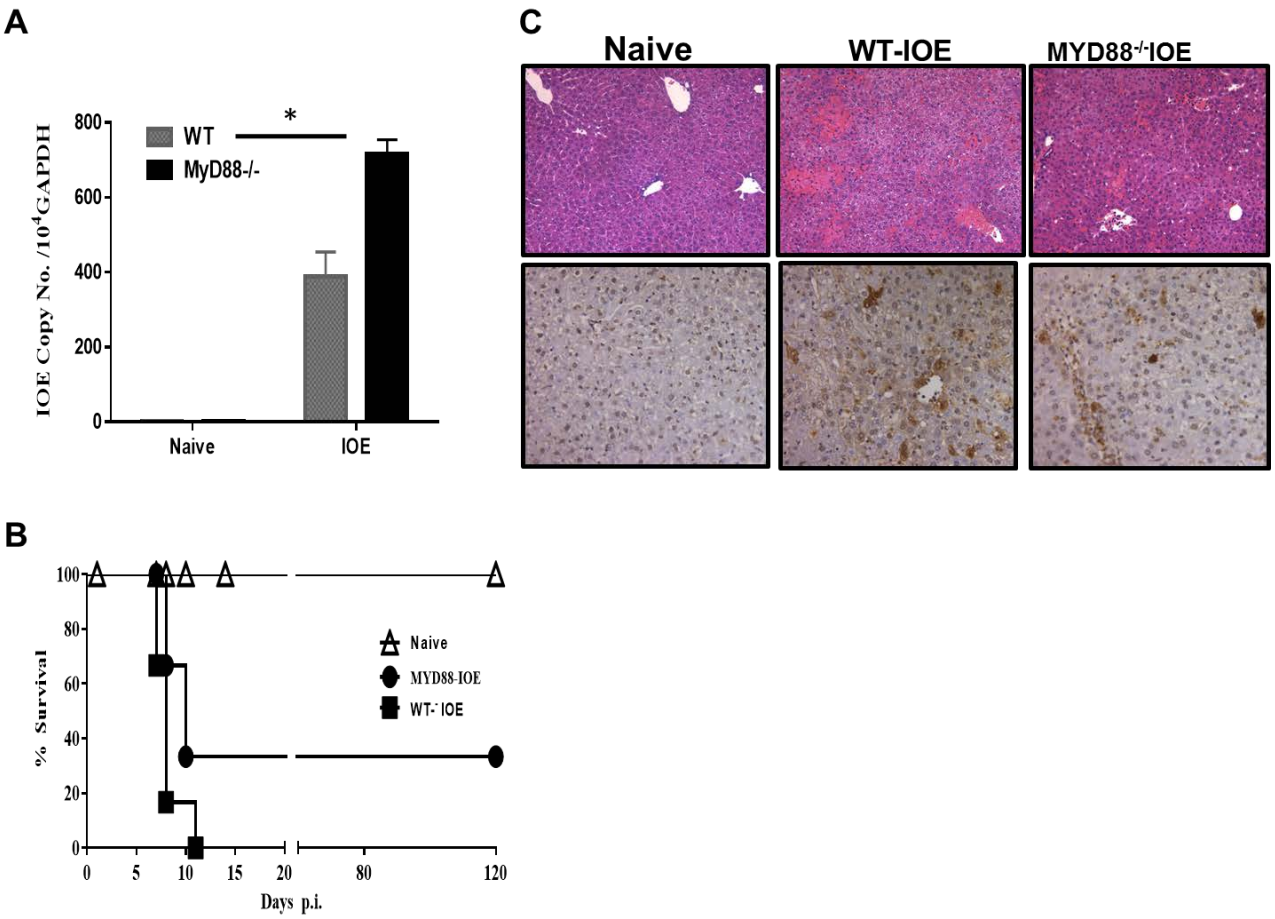

Figure 1. MyD88 deficiency increases IOE bacterial burden but increases survival and reduces liver pathology. A) IOE infected MyD88 mice show a significantly higher IOE copy number than Wt mice. B) IOE infected MyD88 deficient mice have an improved survival rate when compared to infected Wt mice. C) TUNEL staining of *murine* liver tissue showing that MyD88 deficiency attenuates IOE mediated liver pathology when compared to infected Wt mice. Error bars represent standard deviation of the mean. Asterisks represent p values below 0.05.

3.2 MYD88 PROMOTES CANONICAL INFLAMMASOME ACTIVATION IN MACROPHAGES

We examined the contribution of MyD88 to inflammasome activation during IOE infection. To this end, we measured the expression of active caspase-1 in the liver lysates from WT and MyD88$^{-/-}$ mice by immunoblotting. IOE infection elicited inflammasome activation in the liver of WT mice as evidenced by increased caspase 1 activation (Fig. 2A), and high IL-1β serum levels on day 7 p.i. (Fig. 2B). In contrast, MyD88 deficiency inhibited caspase-1 activation in the liver tissues (Fig. 2A) and decreased serum levels of IL-1β (Fig. 2B). These data suggested that MyD88 mediates *Ehrlichia*-induced inflammasome activation.

IOE triggered production of canonical NF-κB-dependent cytokines and the inflammasome-independent cytokine TNF-α in serum (Fig. 2C) and BMMs (Fig. 2D) in a MyD88 dependent manner. IOE infection induced MyD88 dependent activation of caspase-1 and secretion of IL-1β and IL-1α in BMMs (Fig. 2A, 2E, 2F). Secretion of IL-1β is considered a marker of non-canonical inflammasome activation mediated by active caspase 1 and caspase 11.

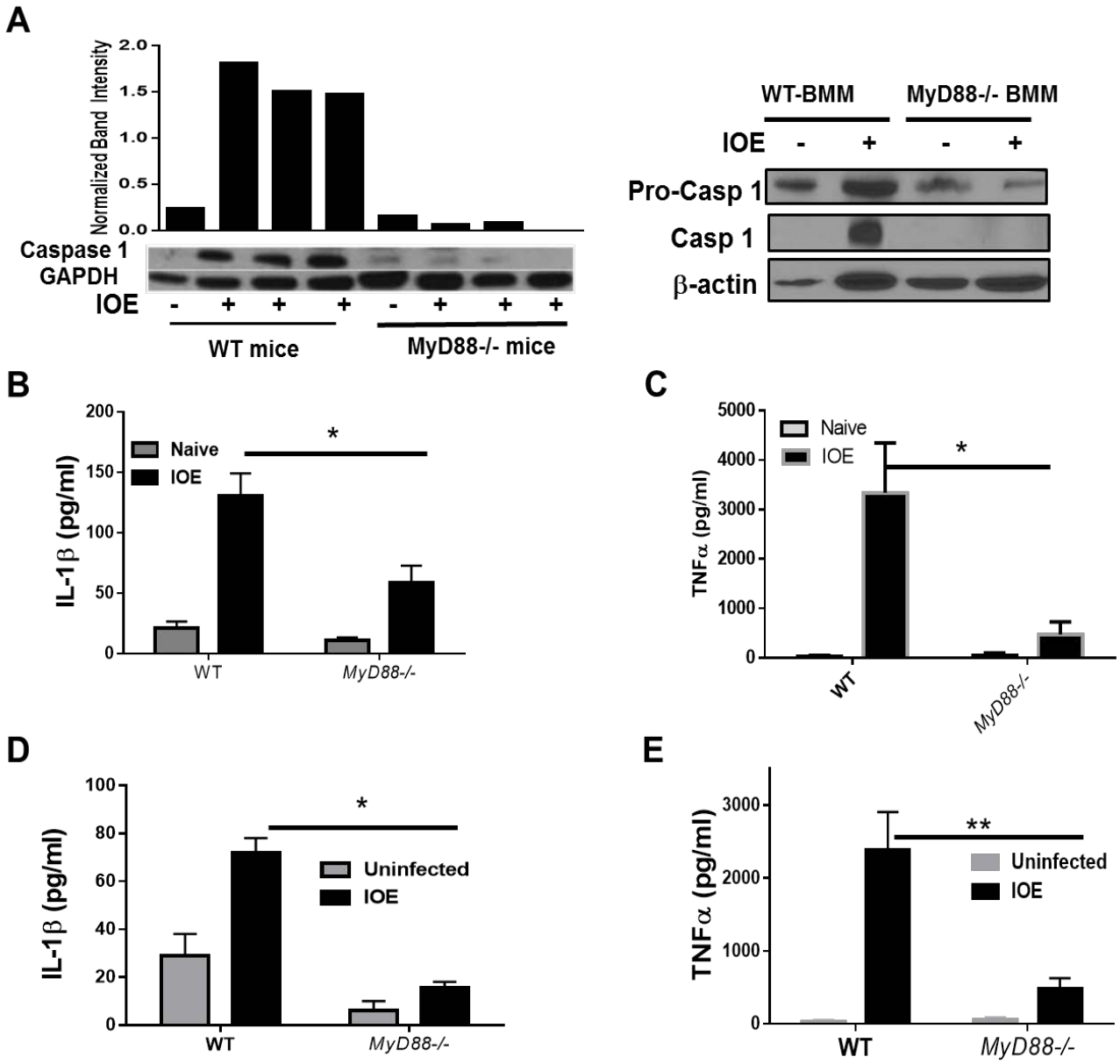

Figure 2. MyD88 is necessary for IOE mediated inflammasome activation. A) IOE infection induces a caspase 1 that is abrogated in MyD88 deficient mice, both *in vivo* from liver lysates and *in vitro* from bone marrow macrophages (BMM). B) IOE infection increases IL-1β C) and TNF-α production *in vivo*, and these increases are reduced in MyD88 deficient mice as determined by immunosorbent assay with serum collected from infected and naïve mice at 7 days post infection. D) IOE infection increases IL-1β E) and TNF-α production *in vitro* using bone marrow derived macrophages from Wt mice. These increases are reduced in cells from MyD88 deficient mice. Error bars express standard deviation of the mean. Asterixis indicate a p value below 0.05.

3.3 MYD88 INHIBITS AUTOPHAGY INDUCTION IN INFECTED MACROPHAGES

Heightened susceptibility of mice to fatal *ehrlichiosis* is associated with suppression of autophagy initiation in liver [30]. Thus, we hypothesized that MyD88 could promote inflammasome activation *in vivo* via autophagy regulation. To test this hypothesis, we examined LC3 II accumulation in infected liver tissues from IOE-infected mice by immunoblotting. Compared to uninfected WT mice, liver lysates from IOE-infected WT mice, on day 7 p.i. showed reduced LC3II conversion and thus a lower LC3II: I ratio (Fig. 3A). Liver lysates from IOE-infected MyD88$^{-/-}$ mice expressed more LC3II, and thus had a higher LC3II:I ratio than naïve MyD88$^{-/-}$ or infected WT mice**.** This suggests that IOE mediates autophagy inhibition, partially via MyD88 signaling.

Next, we examined autophagy induction and flux in infected macrophages from WT and MYD88$^{-/-}$ mice. Consistent with *in vivo* data, IOE infection of WT-BMMs failed to induce LC3 conversion from I to II (Fig. 3B), while infection of MYD88$^{-/-}$ BMMs increased LC3 conversion it decreased LC3II conversion in the liver lysates and BMMs from IOE-infected WT, but not in MYD88$^{-/-}$, mice could be due to defective initiation of autophagy or enhanced autophagosomal degradation. To differentiate between these processes, we examined expression of beclin-1 as a key protein in the initiation of autophagosome formation [31-33]. Our data showed similar beclin-1 expression in IOE-infected WT BMM 24hr p.i. when compared to naïve cells (Fig. 3C).

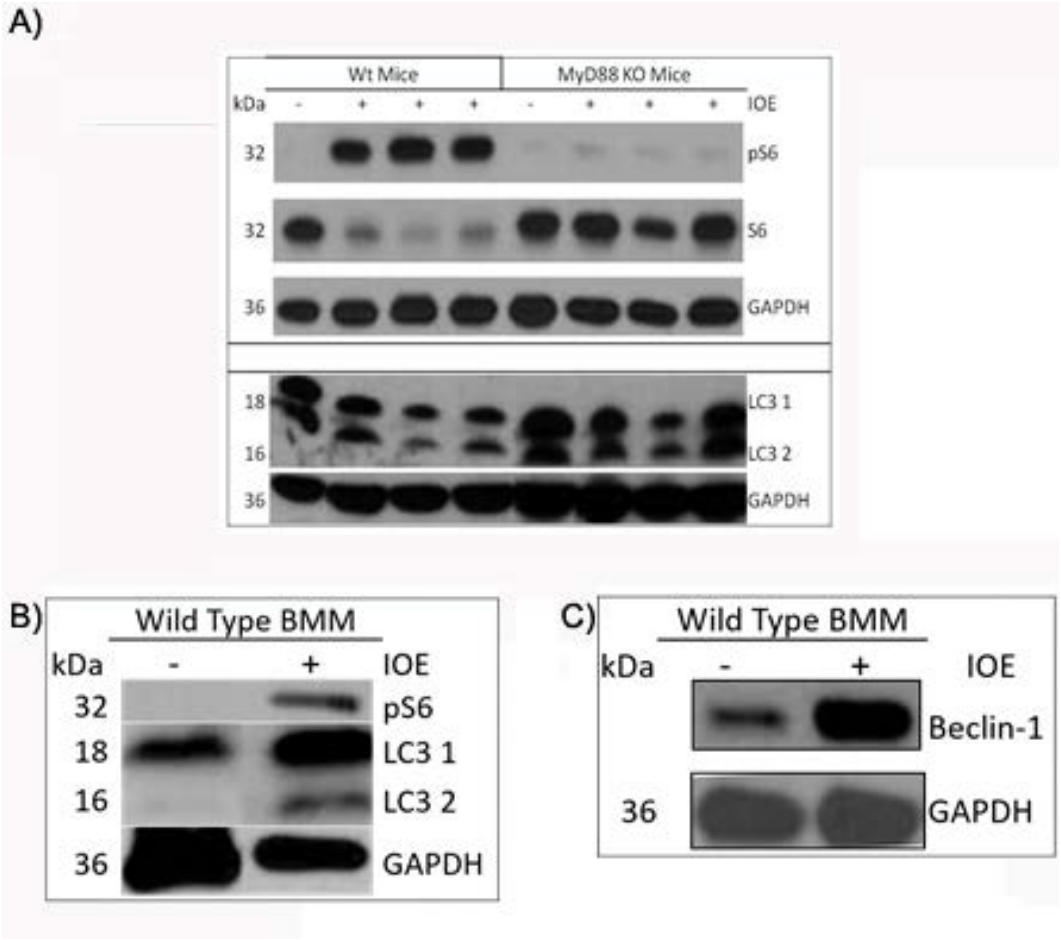

Figure 3. MyD88 is necessary for IOE mediated autophagy regulation via mTORC1. A) Phosphorylation of mTORC1 activation marker Ribosomal S6 (1:5000, Cell Signaling) is increased IOE infection (moi 1/20), and this affect is abrogated in MyD88 deficient mice. Conversion of LC3 II (1:1000, Sigma Aldrich) is reduced *in vivo* with IOE infection, but accumulates in MyD88 deficient mice regardless of IOE infection. B) S6 Phosphorylation is increased, and conversion of LC3 I to II is reduced in cultured bone marrow derived macrophages with IOE infection. C) Beclin I (1:1000, Cell Signaling) accumulates with IOE infection.

To determine whether autophagosomal-lysosomal fusion was occurring confocal microscopy was performed. IOE infected cells were stained for LC3 and the lysosomal pH marker LysoTracker Deep Red. Infected WT BMMs, exhibited LC3 puncta formation, but very little co-localized with the lysosome (shown as yellow), which indicated fusion (Fig. 4). Both puncta formation and fusion were far lower during IOE infection than that induced by LPS stimulation. This suggests that absence of LPS in *Ehrlichia* may provide an immune evasion strategy. These data re-enforce the conclusion that IOE infection inhibits autophagosome-lysosomal fusion in macrophages.

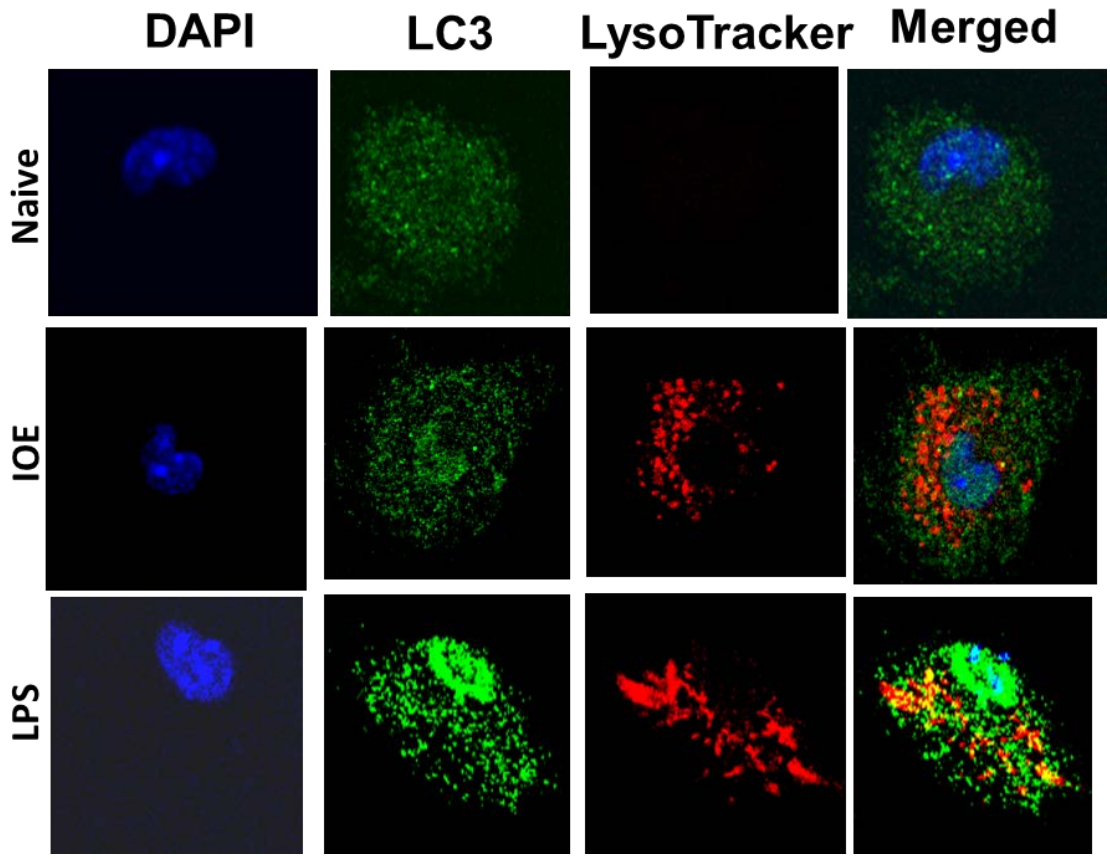

Figure 4. Autophagy flux is reduced during IOE infection compared to LPS control. Confocal microscopy (100x) showing immunofluorescent staining of bone marrow derived macrophages for LC3 (1:200) and lysosomal pH (LysoTracker Deep Red) during IOE infection (moi 1/20) and when stimulated with LPS control (200 ng/mL). Co-localization of active lysosomes and LC3 puncta indicate autophagosomal-lysosomal fusion.

3.4 MYD88-MEDIATED INHIBITION OF AUTOPHAGY INDUCTION IN INFECTED MACROPHAGES IS MEDIATED VIA MTORC1 ACTIVATION

Activation of mTORC1 negatively regulates autophagy [34]. To investigate the mechanism of MyD88-dependent autophagy inhibition during IOE infection, we first examined mTORC1 activation *in vivo*. mTORC1 activation is measured by phosphorylation of its downstream target ribosomal protein S6 (pS6). Infected WT mice had elevated pS6 in the liver on day 7 p.i., while infected MyD88$^{-/-}$ mice lacked pS6 at the same time point (Fig. 3A).

To confirm the *in vivo* data**,** we examined mTORC1 activation in *in vitro* infected BMMs**.** Immunoblotting revealed a clear increase in pS6 in infected Wt BMMs post infection, consistent with the *in vivo* findings (Fig. 3B).

3.5 VIRULENT *EHRLICHIA* INDUCES MITOCHONDRIAL DAMAGE AND MYD88-DEPENDENT P62 ACCUMULATION IN MACROPHAGES.

LPS stimulation of macrophages induces NF-κB-dependent p62 accumulation, promoting elimination of damaged mitochondria and preventing inflammasome activation [35-37]. Thus, we hypothesized that MyD88-mediated inflammasome activation in macrophages and liver injury following IOE infection is due to defective mitophagy. To test this hypothesis, began by examining the ultrastructure of infected cells using transmission electron microscopy (TEM). Our data indicated that infected WT BMMs had fewer double-membrane autophagosomes and autolysosomes, and damaged mitochondria when compared to uninfected WT BMMs (Fig. 5A).

These data suggest that IOE infection induces mitochondrial damage in macrophages that fail to be eliminated due to inhibition of autophagy flux and thus mitophagy.

To confirm IOE mediated mitochondrial damage we stained BMMs for p62 and the mitochondrial marker MitoTracker Deep Red. Immunofluorescence staining demonstrated an increased in p62 puncta in infected WT-BMMs, but decreased colocalization with the mitotracker when compared to LPS control (Fig. 5B). Though p62 levels appear lover in immunofluorescent imaging, immunoblotting demonstrated that uninfected and IOE-infected WT BMMs expressed similar levels of p62 (Fig. 5C). However, p62 levels were significantly lower in IOE-infected MyD88$^{-/-}$ BMMs compared to infected WT BMMs and uninfected MyD88$^{-/-}$BMMs (Fig. 5C). We postulated that decreased p62 in infected MyD88$^{-/-}$ BMMs could be the results of rapid degradation via autophagy flux [35, 38, 39]. Alternatively, it is possible that decreased NF-κB activation, secondary to MyD88 deficiency, could account for decreased p62. To test this, we measured the expression of phosphorylated p38 mitogen-activated protein kinase (MAPK), as a marker of NF-κB activation [40]. The expression of p38 MAPK was indeed abolished in MyD88$^{-/-}$ BMMs (Fig. 5D), suggesting that MyD88-dependent NF-κB activation in infected macrophages could contribute to decreased p62 in MyD88$^{-/-}$ BMMs.

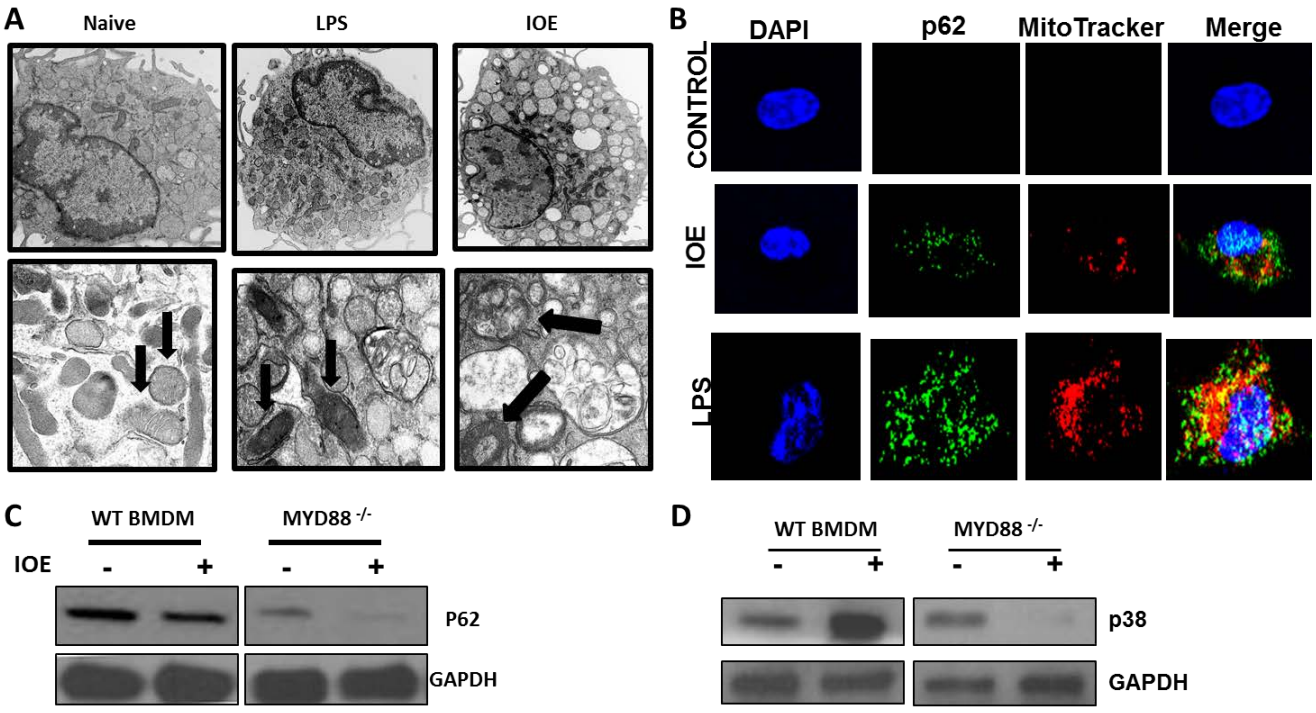

Figure 5. IOE infection induces mitochondrial damage. A) Electron microscopy of bone marrow derived macrophages showing that IOE (moi 1/20) increases autophagosome formation and mitochondrial damage in similar manner to LPS (200 ng/mL) control. B) Fluorescent microscopy (100X) staining for p62 (1:50 Cell Signaling) and MitroTracker Deep Red. Colocalization of mitochondria and the ubiquitination marker p62 indicate damaged mitochondria. C) Levels of p62 remain steady with IOE infection in Wt cells, but reduce with MyD88 deficiency, potentially indicating a reduction in damaged cell components or an increase in degradation. D) Levels of p38 (1:1000, Cell Signaling) increase with IOE infection in WT BMM, but decrease with IOE infection in MyD88-/- BMM.

3.6 TLR9 IS THE UPSTREAM SIGNAL THAT MEDIATES MYD88-DEPENDENT MTORC1 ACTIVATION AND INFLAMMASOME ACTIVATION.

Virulent IOE infection triggers upregulation of several TLRs in liver tissue of infected mice including TLR2, TLR7, and TLR9 [3]. To determine the TLR that mediates MyD88-dependent mTORC1 and inflammasome activation, we compared IL-1β production and expression of pS6 in BMMs from TLR2$^{-/-}$, TLR7$^{-/-}$, and TLR9$^{-/-}$ mice to that expressed in WT BMMs. Infection of TLR2$^{-/-}$ and TLR7$^{-/-}$ BMMs elicited IL-1β, albeit at slightly lower levels than WT BMMs (Fig. 6A). In contrast, infection of TLR9$^{-/-}$ BMMs did not elicit IL-1β production, and abrogated infection induced S6 phosphorylation when compared to WT, TLR2$^{-/-}$, or TLR7$^{-/-}$ macrophages (Fig. 6B). Thus, these data suggest that TLR9 is the major upstream pathway that mediates MyD88-dependent activation of mTORC1 and inflammasome activation during *Ehrlichia* infection.

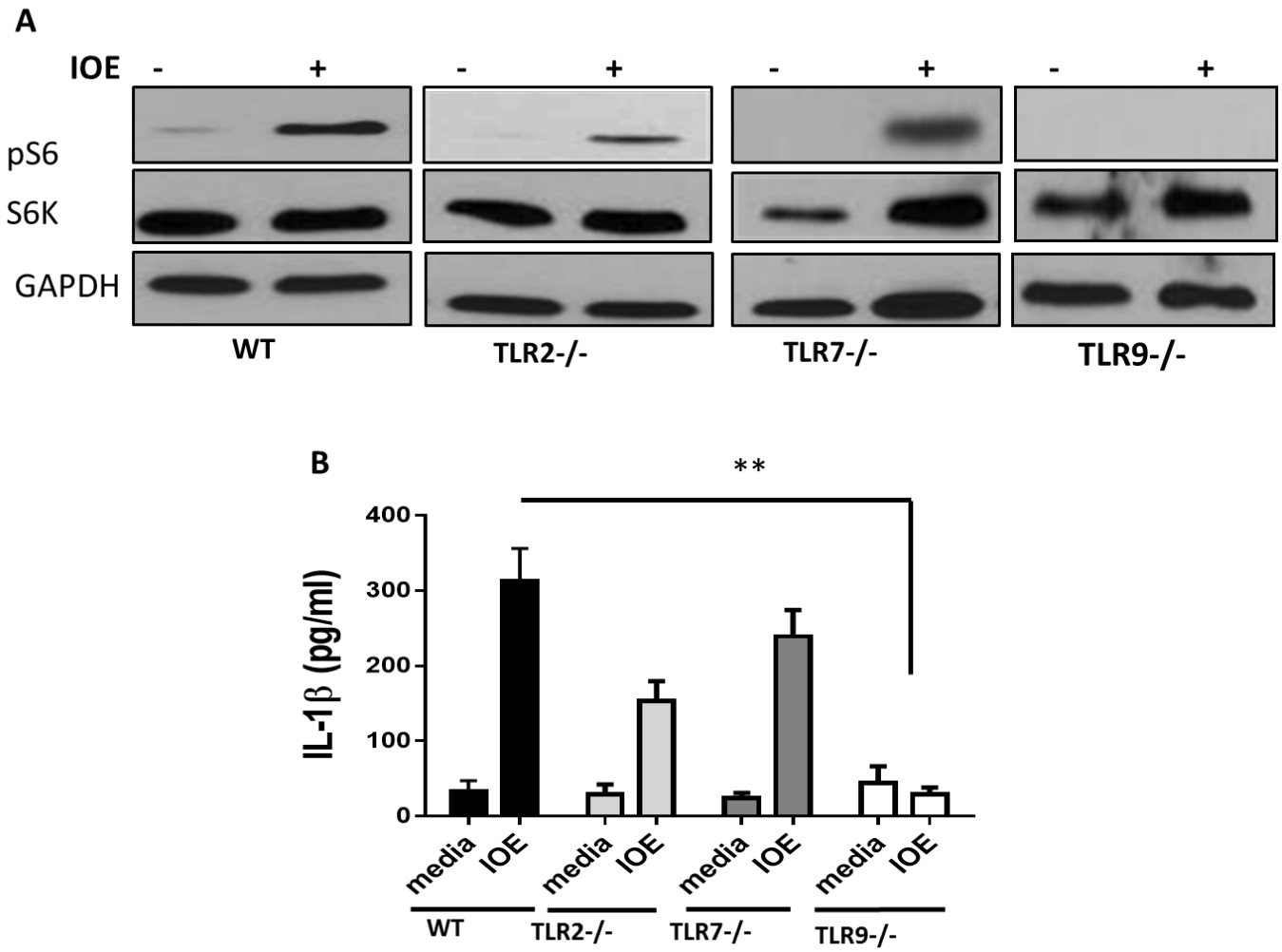

Figure 6. IOE mediated autophagy regulation and inflammasome activation is TLR 9 dependent. A) Immunoblot analysis for ribosomal S6 phosphorylation (1:5000, Cell Signaling) in wild-type, TLR2-/-, TLR7-/-, and TLR9$^{-/-}$ murine bone marrow derived macrophage lysates at 24 hr post IOE (moi 1/20) infection. Left margin, molecular size in kilodaltons (kDa). B) IL-1β (pg/mL) in WT and TLR9-/- BMM cell supernatants infected with IOE (moi 20) and stimulated with IFN-β (400 units/mL) determined by ELISA. Error bars express standard deviation of the mean. Asterix indicate a p value below 0.05.

To further investigate the role of TLR9 in IOE infection we compared expression of phosphorylated S6 and production of IL-1β in BMMs from IOE infected TLR9$^{-/-}$ mice which had also been stimulated with IFN-β, and compared the response to WT BMMs. Interestingly, attenuation S6 phosphorylation and reduced IL-1β secretion in TLR9$^{-/-}$ BMMs compared to Wt BMM occurred even with the addition of IFN-β (Fig 7A, B). Abrogation of S6 phosphorylation even occurred during LPS stimulation. These data indicate that TLR9 is the major upstream pathway that mediates MYD88-dependent activation of mTORC1 and autophagy inhibition during *Ehrlichia* infection, which in turn elicits inflammasome activation.

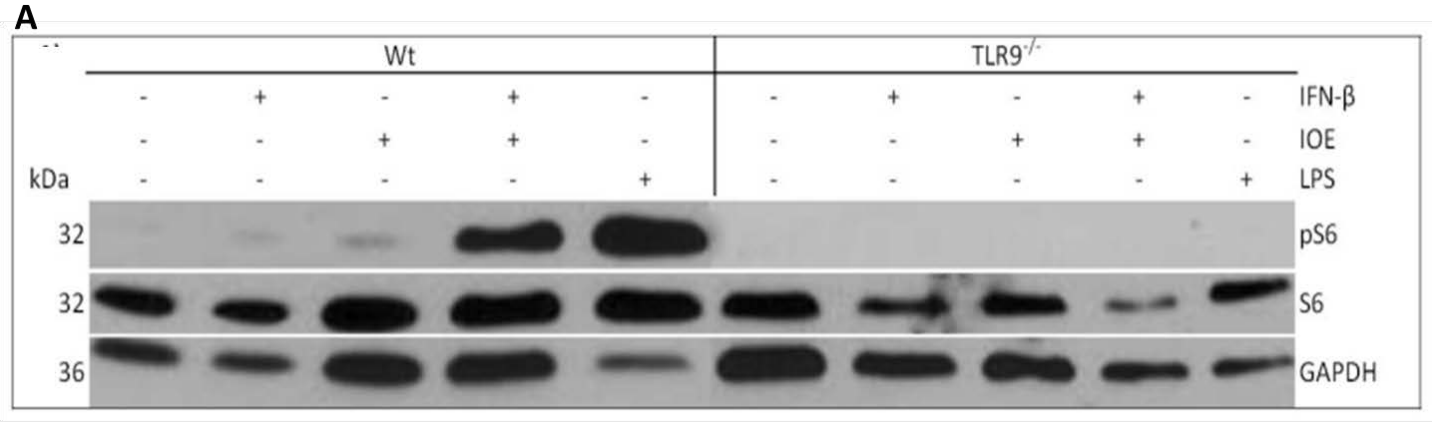

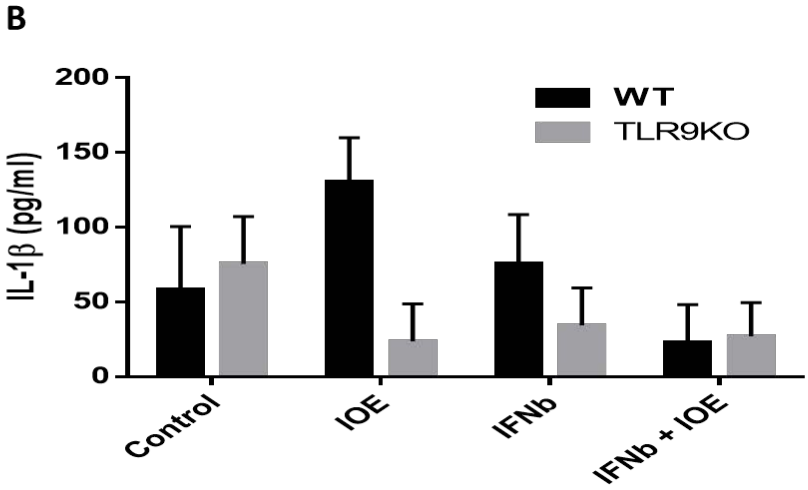

Figure 7. **IOE, IFN-β, and LPS mediated autophagy regulation and inflammasome activation is TLR 9 dependent.** A) Immunoblot analysis for ribosomal S6 phosphorylation (1:5000, Cell Signaling) in wild-type and TLR9$^{-/-}$ murine bone marrow derived macrophage lysates with and without IFN-β (400 units/mL), IOE (moi 20), and LPS (1μg/mL) stimulation for 24 hours. Left margin, molecular size in kilodaltons (kDa). B) IL-1β (pg/mL) in WT and TLR9-/- BMM cell supernatants infected with IOE (moi 1/20) and stimulated with IFN-β (400 units/mL) determined by ELISA. Error bars express standard deviation of the mean.

3.7 IFNB ACTS AS AN AUTOPHAGY SUPPRESSOR DURING VIRULENMT *EHRLICHIA* INFECTION

Our previous work has shown that IFN mRNA levels vary between the *Ehrlichia* strains IOE and EM, with the more virulent IOE showing much higher IFN mRNA levels. This is differential IFN expression is supported by serum IFN levels detected in serum taken from *in vivo murine* IOE and EM infection over a 7-day time course (Fig. 7B). These data demonstrate that the variation in IFN mRNA expression between IOE and EM *Ehrlichia* strains is perpetuation into translation, verifying a physiologically relevant change.

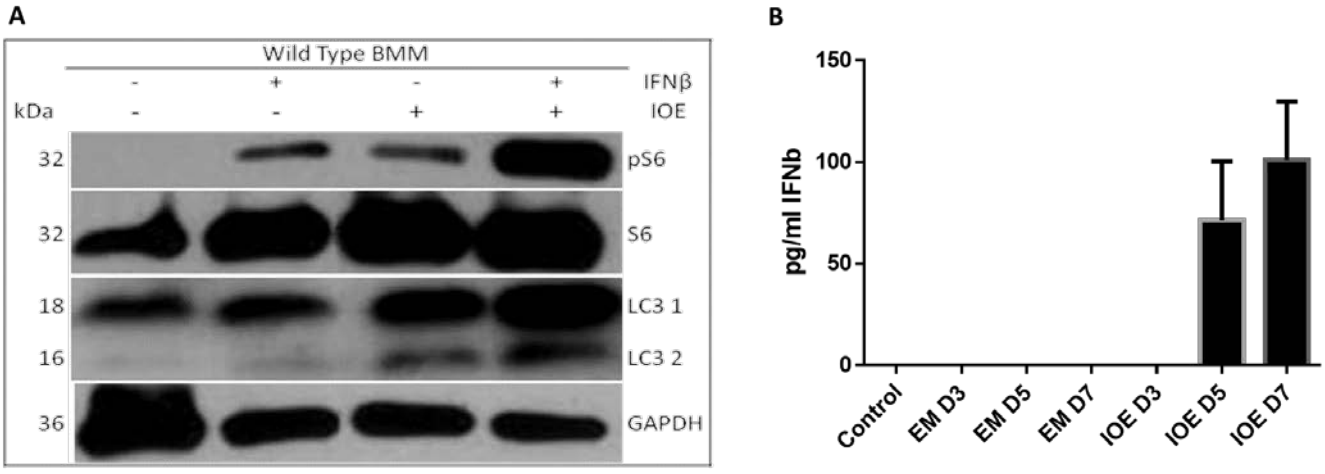

Figure 8. IFNβ plays a role in IOE mediated autophagy regulation. A) Phosphorylation of mTORC1 marker ribosomal S6 (1:5000, Cell Signaling), and LC3 I:II conversion (Sigma Aldrich 1:1000) indicating that IFNβ (400 units / mL) is needed to fully recapitulate *in vivo* IOE (moi 1/20) mediated mTORC1 activity. B) IFNβ (pg/mL) levels determined from serum of EM and IOE i.p. infected mice at 3, 5, and 7 days post infection using ELISA. Data indicate that IFNβ levels rise only in the virulent IOE, and only as mice approach the terminal end of infection.

3.8 EFFECT OF INFECTION WITH EXTRACELLULAR BACTERIA ON AUTOPHAGY IN MURINE MACROPHAGES

As our study depends on the use of *Ehrlichia* as a broad model for innate immune response, we used the bacteria *Staphylococcus aureus* (Fig. 9A) and *Acinetobacter baumannii* (Fig. 9B) at a series of multiplicity of infections (MOI) and time points to test the autophagy response *in vitro* with protein from infected *murine* bone marrow derived macrophages. Here both the increased S6 phosphorylation and low LC3 II:I ratio observed with IOE also occur during both *A. baumannii* and *S. aureus* infection.

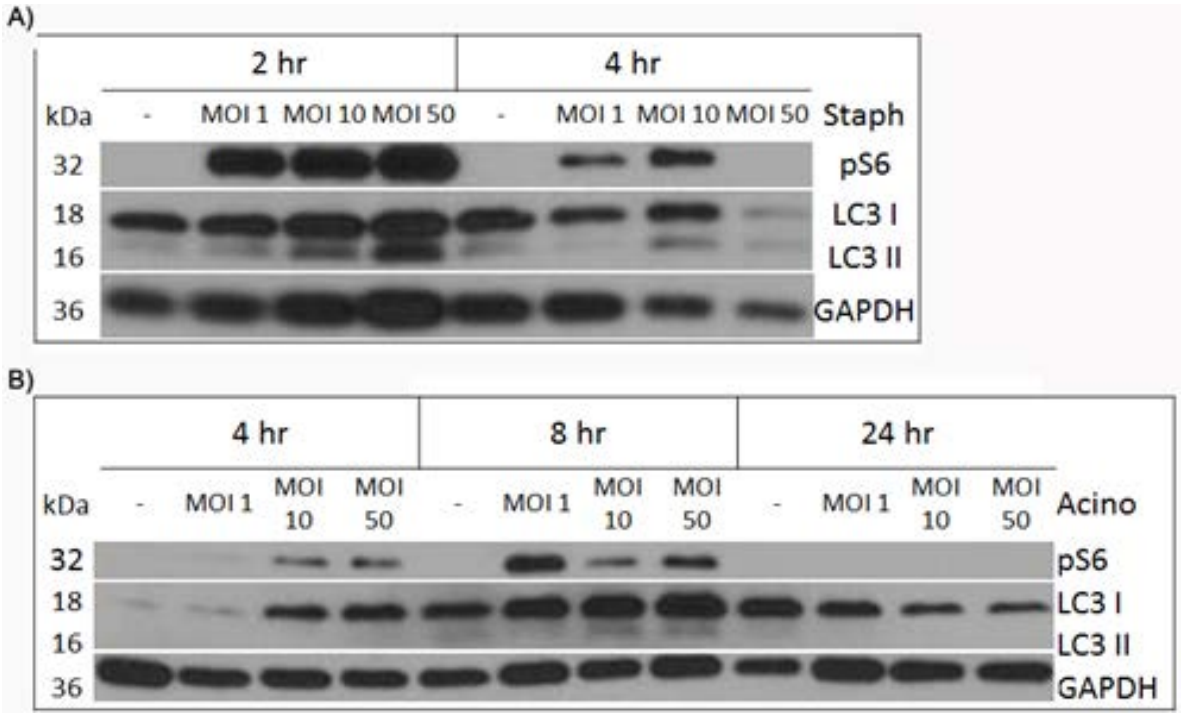

Figure 9. Extracellular infection shows similar autophagy response in murine BMM. Ribosomal S6 phosphorylation (1:5000 Cell Signaling) and LC3 I and II (1:1000 Sigma Aldrich) levels in murine bone marrow derived macrophages infected with 1, 10, or 50 moi *S. aureus* or *A. baumannii* collected at 2, 4, 8, or 24 hours to assess kinetic autophagy progression.

4.0 DISCUSSION

Ehrlichia infection induces deleterious inflammasome activation, which contributes to excessive inflammation and organ damage in the murine model of fatal ehrlichiosis. However, the downstream adaptor molecules that mediate signaling during *Ehrlichia* infection as well as the molecular mechanisms that regulate inflammasome activation during infection with *Ehrlichia* remain unknown. MYD88 signaling functions as an immune evasion mechanism, inhibiting mTORC1 dependent autophagy and inducing inflammasome activation. These data are consistent with the previously established deficiency in *E. muris* clearance from MyD88 deficient mice [41] [42]. We have also shown that virulent IOE triggers inflammasome activation marked by upregulation of NLRP3, cleavage of caspase 1, and secretion of IL-1β [3, 27]. We demonstrate that MYD88 signaling contributes to caspase 1 activation and IL-1β secretion *in vivo* and *in vitro* in infected macrophages.

Autophagy is a critical innate immune defense mechanism against several facultative intracellular bacterial pathogens such as Legionella and Salmonella. However, the role of autophagy in protective innate immunity against infection with obligate intracellular virulent bacteria such as *Ehrlichia* is not clearly defined. Autophagy does have an established negative correlation with inflammasome activation currently ties to its role in the elimination of both microbial and host danger ligands that activate inflammasome complexes [43]. We show that IOE-induced MYD88 signaling blocks autophagy via activation of the mTORC1 pathway.

Additionally, we found that TLR9 is a key upstream receptor for IOE mediated autophagy suppression during virulent *Ehrlichia* infection. Though it is not yet clear how TLR9 is triggered during virulent *Ehrlichia* infection, it is possible that TLR9 is responding to DAMPs [15] released as a result of IOE mediated cell damage as well as responding to IOE DNA directly. TLR9 activation, in *murine* bone marrow derived macrophages, is essential for IOE mediated mTORC1 activation. This mTORC1 activation suppresses the canonical mTORC1 dependent autophagy, and results in DAMP accumulation that can release TLR9 activating DAMPS and result in a positive feedback loop of reinforced mTORC1 activation (Fig. 10). This positive feedback loop would minimize potential *Ehrlichia* degradation in the cell. Surprisingly, lack of TLR9 both abrogated mTORC1 activation and attenuated IL-1β secretion in response to IOE infection as well as LPS and IFNβ stimulation when compared to WT-BMMs (Fig. 7). Our model uniquely highlights a novel mechanism for regulation of autophagy and inflammasome activation during infection. Future studies will define key host and/or microbial molecules that induce TLR9/MYD88-mediated mTORC1-dependent autophagy inhibition and inflammasome activation during infection with LPS-negative *Ehrlichia*.

The balance between protective immunity and immunopathology during *Ehrlichia* infection determines outcome. In this study, we demonstrate that autophagy is not only a host-protective mechanism that mediates elimination of *Ehrlichia*, but is also critical for clearance of damaged mitochondria through mitophagy. Indeed, elimination of damaged mitochondria is important to maintain cellular homeostasis and prevent excessive inflammation and cellular injury. Virulent IOE infection induces mitochondrial damage in both macrophages and hepatocytes. *Ehrlichia chaffeensis,* a strain closely related to IOE, inhibits mitochondrial activities and metabolism [44, 45]. *Ehrlichia* harbor several effector proteins that are secreted via

type I and IV secretion systems [46]. These proteins are translocated from the bacterium residing in the phagosome into the host cell cytoplasm and localized to the mitochondria [44]. It has been shown that upregulation of mitochondrial manganese superoxide dismutase (MnSOD) within *E. chaffeensis* infected macrophages prevent reactive oxygen species (ROS)-induced cellular damage and apoptosis. *E. chaffeensis* causes mild disease in WT mice. Thus, it is possible that infection with virulent IOE causes mitochondrial damage in infected macrophages by increasing ROS without inducing MnSOD[46]. Nevertheless, we show here that MyD88 blocks mitochondrial autophagy in macrophages by blocking autophagy flux and co-localization of p62 with damaged mitochondria. Further, lack of p62 degradation in infected cells may result in further cytotoxicity. Indeed, attenuated apoptosis and necrosis of hepatocytes and Kupffer cells in the liver of IOE-infected MyD88$^{-/-}$ mice further suggest that MyD88 induces liver injury via inhibition of autophagy induction and flux in macrophages and inhibition of mitophagy in hepatocytes.

The *Ehrlichia* ligand that triggers host-pathogenic inflammasome activation remains elusive. Though *Ehrlichia* tandem repeat proteins (TRPs) and type I and IV secretion system effectors are potential candidates for activation, secretion of these proteins into host cell cytosol [47] would enable them to trigger cytosolic NLRs. Alternatively, accumulation of mitochondrial DNA (mtDNA) or increased reactive oxygen species (ROS) in IOE- infected macrophages could act as DAMPS responsible for inflammasome activation. In support of this conclusion, our data show that MyD88-dependent mTORC1 activation is mediated via TLR9, an endosomal TLR that is triggered by microbial or host DNA including mtDNA. On the other hand, our data show that blocking bacterial internalization by Dynasore treatment abrogates mTORC1 activation in

infected macrophages, suggesting that TLR9 signals and subsequent mTORC1 activation are also triggered, by microbial DNA or DNA-binding *Ehrlichia* protein.

This is the first study to reveal a novel mechanism whereby virulent *Ehrlichia* exploits the MyD88-mTORC1-autophagy pathway to: evade host innate immune responses, elicit host-pathogenic inflammasome activation, induce inflammatory macrophage death, and induce liver injury. Inhibition of autophagy in macrophages, the main target cells, together with induction of host cell death enhances not only intracellular bacterial survival, but also dissemination and multi-organ injury. Our results highlight a potential role for mitochondrial damage in *Ehrlichia*-induced macrophage death. In conclusion, this study shows, for the first time, that obligate intracellular *Ehrlichia* exploits the AKT-mTORC1 pathway to evade autophagy and intracellular killing. Our current working model proposes that signaling via TLR9 and MyD88 elicit mTORC1 activation, which blocks autophagy initiation in macrophages and hinders adaptive immunity against *Ehrlichia* (Fig. 10). Thus, targeting the mTORC1 pathway and identifying key PAMPs and DAMPs that induce MyD88 signaling, autophagy inhibition and inflammasome activation provides novel therapeutic approaches for the treatment and prevention of this important disease.

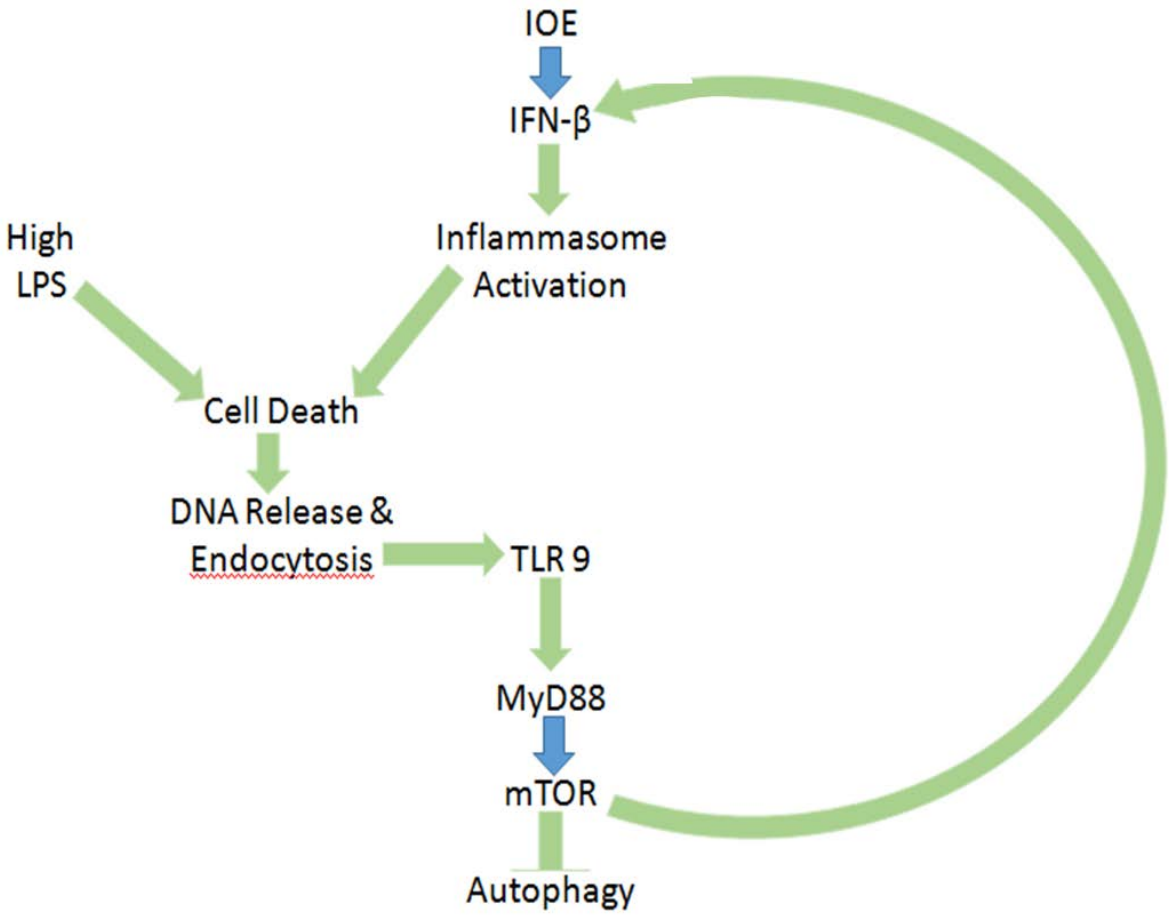

Figure 10. Working hypothesis. Summary figure showing that IFNβ seems to be acting upstream of TLR9, MyD88, and mTORC1 activation in macrophages. This activation may be tied to DAMP and PAMP production during the inflammatory response, and does not address the mechanism for production of initial IFN-β.

5.0 BIBLIOGRAPHY

1. Walker, D.H., C.D. Paddock, and J.S. Dumler, *Emerging and re-emerging tick-transmitted rickettsial and ehrlichial infections.* Med Clin North Am, 2008. **92**(6): p. 1345-61, x.
2. Olano, J.P. and D.H. Walker, *Human ehrlichioses.* Med Clin North Am, 2002. **86**(2): p. 375-92.
3. Chattoraj, P., et al., *TLR2 and Nod2 mediate resistance or susceptibility to fatal intracellular Ehrlichia infection in murine models of ehrlichiosis.* PLoS One, 2013. **8**(3): p. e58514.
4. Walker, D.H. and J.S. Dumler, *Human monocytic and granulocytic ehrlichioses. Discovery and diagnosis of emerging tick-borne infections and the critical role of the pathologist.* Arch Pathol Lab Med, 1997. **121**(8): p. 785-91.
5. Luo, T., et al., *Ehrlichia chaffeensis Exploits Canonical and Noncanonical Host Wnt Signaling Pathways To Stimulate Phagocytosis and Promote Intracellular Survival.* Infect Immun, 2015. **84**(3): p. 686-700.
6. Fichtenbaum, C.J., L.R. Peterson, and G.J. Weil, *Ehrlichiosis presenting as a life-threatening illness with features of the toxic shock syndrome.* Am J Med, 1993. **95**(4): p. 351-7.
7. Lin, M. and Y. Rikihisa, *Obligatory intracellular parasitism by Ehrlichia chaffeensis and Anaplasma phagocytophilum involves caveolae and glycosylphosphatidylinositol-anchored proteins.* Cell Microbiol, 2003. **5**(11): p. 809-20.
8. Ismail, N., et al., *Overproduction of TNF-alpha by CD8+ type 1 cells and down-regulation of IFN-gamma production by CD4+ Th1 cells contribute to toxic shock-like syndrome in an animal model of fatal monocytotropic ehrlichiosis.* J Immunol, 2004. **172**(3): p. 1786-800.
9. Davis, B.K., H. Wen, and J.P. Ting, *The inflammasome NLRs in immunity, inflammation, and associated diseases.* Annu Rev Immunol, 2011. **29**: p. 707-35.
10. Maverakis, E., et al., *Glycans in the immune system and The Altered Glycan Theory of Autoimmunity: a critical review.* J Autoimmun, 2015. **57**: p. 1-13.
11. Seong, S.Y. and P. Matzinger, *Hydrophobicity: an ancient damage-associated molecular pattern that initiates innate immune responses.* Nat Rev Immunol, 2004. **4**(6): p. 469-78.
12. Broz, P. and V.M. Dixit, *Inflammasomes: mechanism of assembly, regulation and signalling.* Nat Rev Immunol, 2016. **16**(7): p. 407-20.
13. Vigano, E., et al., *Human caspase-4 and caspase-5 regulate the one-step non-canonical inflammasome activation in monocytes.* Nat Commun, 2015. **6**: p. 8761.

14. Wang, J.Q., et al., *Toll-Like Receptors and Cancer: MYD88 Mutation and Inflammation.* Front Immunol, 2014. **5**: p. 367.
15. Bao, W., et al., *Toll-like Receptor 9 Can be Activated by Endogenous Mitochondrial DNA to Induce Podocyte Apoptosis.* Sci Rep, 2016. **6**: p. 22579.
16. Re, F. and J.L. Strominger, *Monomeric recombinant MD-2 binds toll-like receptor 4 tightly and confers lipopolysaccharide responsiveness.* J Biol Chem, 2002. **277**(26): p. 23427-32.
17. Kim, K.H. and M.S. Lee, *Autophagy--a key player in cellular and body metabolism.* Nat Rev Endocrinol, 2014. **10**(6): p. 322-37.
18. Chauhan, S., et al., *Pharmaceutical screen identifies novel target processes for activation of autophagy with a broad translational potential.* Nat Commun, 2015. **6**: p. 8620.
19. Mizushima, N. and T. Yoshimori, *How to interpret LC3 immunoblotting.* Autophagy, 2007. **3**(6): p. 542-5.
20. Klionsky, D.J., et al., *Guidelines for the use and interpretation of assays for monitoring autophagy in higher eukaryotes.* Autophagy, 2008. **4**(2): p. 151-75.
21. Kim, K.H. and M.S. Lee, *Autophagy as a crosstalk mediator of metabolic organs in regulation of energy metabolism.* Rev Endocr Metab Disord, 2014. **15**(1): p. 11-20.
22. Li, Q., Y. Liu, and M. Sun, *Autophagy and Alzheimer's Disease.* Cell Mol Neurobiol, 2016.
23. Kissing, S., et al., *Disruption of the vacuolar-type H+-ATPase complex in liver causes MTORC1-independent accumulation of autophagic vacuoles and lysosomes.* Autophagy, 2017: p. 0.
24. Lv, S., et al., *Dissection and integration of the autophagy signaling network initiated by bluetongue virus infection: crucial candidates ERK1/2, Akt and AMPK.* Sci Rep, 2016. **6**: p. 23130.
25. Alves, R.N., et al., *The spreading process of Ehrlichia canis in macrophages is dependent on actin cytoskeleton, calcium and iron influx and lysosomal evasion.* Vet Microbiol, 2014. **168**(2-4): p. 442-6.
26. Cardenas, C. and J.K. Foskett, *Mitochondrial Ca(2+) signals in autophagy.* Cell Calcium, 2012. **52**(1): p. 44-51.
27. Yang, Q., et al., *Type I interferon contributes to noncanonical inflammasome activation, mediates immunopathology, and impairs protective immunity during fatal infection with lipopolysaccharide-negative ehrlichiae.* Am J Pathol, 2015. **185**(2): p. 446-61.
28. Ghose, P., et al., *The interaction between IL-18 and IL-18 receptor limits the magnitude of protective immunity and enhances pathogenic responses following infection with intracellular bacteria.* J Immunol, 2011. **187**(3): p. 1333-46.
29. Yang, Q., P. Ghose, and N. Ismail, *Neutrophils mediate immunopathology and negatively regulate protective immune responses during fatal bacterial infection-induced toxic shock.* Infect Immun, 2013. **81**(5): p. 1751-63.
30. Yang, Q., et al., *Type I Interferon Contributes to Noncanonical Inflammasome Activation, Mediates Immunopathology, and Impairs Protective Immunity during Fatal Infection with Lipopolysaccharide-Negative Ehrlichiae.* Am J Pathol, 2014.
31. Deretic, V., *Autophagy in immunity and cell-autonomous defense against intracellular microbes.* Immunol Rev, 2011. **240**(1): p. 92-104.
32. Amarnath, S., et al., *Rapamycin generates anti-apoptotic human Th1/Tc1 cells via autophagy for induction of xenogeneic GVHD.* Autophagy, 2010. **6**(4): p. 523-41.

33. Alvarado, A.G., et al., *Coordination of self-renewal in glioblastoma by integration of adhesion and microRNA signaling.* Neuro Oncol, 2016. **18**(5): p. 656-66.
34. Tattoli, I., et al., *Bacterial autophagy: the trigger, the target and the timing.* Autophagy, 2012. **8**(12): p. 1848-50.
35. Zhong, Z., et al., *NF-kappaB Restricts Inflammasome Activation via Elimination of Damaged Mitochondria.* Cell, 2016. **164**(5): p. 896-910.
36. Shi, C.S., et al., *Activation of autophagy by inflammatory signals limits IL-1beta production by targeting ubiquitinated inflammasomes for destruction.* Nat Immunol, 2012. **13**(3): p. 255-63.
37. Deretic, V., *Autophagy as an innate immunity paradigm: expanding the scope and repertoire of pattern recognition receptors.* Curr Opin Immunol, 2012. **24**(1): p. 21-31.
38. Legrand-Poels, S., et al., *Free fatty acids as modulators of the NLRP3 inflammasome in obesity/type 2 diabetes.* Biochem Pharmacol, 2014. **92**(1): p. 131-41.
39. He, Q., et al., *Mitochondria-targeted antioxidant prevents cardiac dysfunction induced by tafazzin gene knockdown in cardiac myocytes.* Oxid Med Cell Longev, 2014. **2014**: p. 654198.
40. Kim, H.Y. and Y. Rikihisa, *Roles of p38 mitogen-activated protein kinase, NF-kappaB, and protein kinase C in proinflammatory cytokine mRNA expression by human peripheral blood leukocytes, monocytes, and neutrophils in response to Anaplasma phagocytophila.* Infect Immun, 2002. **70**(8): p. 4132-41.
41. Miura, K., et al., *Ehrlichia chaffeensis induces monocyte inflammatory responses through MyD88, ERK, and NF-kappaB but not through TRIF, interleukin-1 receptor 1 (IL-1R1)/IL-18R1, or toll-like receptors.* Infect Immun, 2011. **79**(12): p. 4947-56.
42. Koh, Y.S., et al., *MyD88-dependent signaling contributes to host defense against ehrlichial infection.* PLoS One, 2010. **5**(7): p. e11758.
43. Yuk, J.M. and E.K. Jo, *Crosstalk between autophagy and inflammasomes.* Mol Cells, 2013. **36**(5): p. 393-9.
44. Liu, Y., et al., *Obligate intracellular bacterium Ehrlichia inhibiting mitochondrial activity.* Microbes Infect, 2011. **13**(3): p. 232-8.
45. Von Ohlen, T., et al., *Identification of critical host mitochondrion-associated genes during Ehrlichia chaffeensis infections.* Infect Immun, 2012. **80**(10): p. 3576-86.
46. Liu, H., et al., *Ehrlichia type IV secretion effector ECH0825 is translocated to mitochondria and curbs ROS and apoptosis by upregulating host MnSOD.* Cell Microbiol, 2012. **14**(7): p. 1037-50.
47. Dunphy, P.S., T. Luo, and J.W. McBride, *Ehrlichia moonlighting effectors and interkingdom interactions with the mononuclear phagocyte.* Microbes Infect, 2013. **15**(14-15): p. 1005-16.